Phase transitions in predator-prey systems

Seido Nagano* and Yusuke Maeda
Department of Bioinformatics, Ritsumeikan University, 1-1-1 Nojihigashi, Shiga 525-8577, Japan
(Received 29 September 2011; published 23 January 2012)

The relationship between predator and prey plays an important role in ecosystem conservation. However, our understanding of the principles underlying the spatial distribution of predators and prey is still poor. Here we present a phase diagram of a predator-prey system and investigate the lattice formation in such a system. We show that the production of stable lattice structures depends on the limited diffusion or migration of prey as well as higher carrying capacity for the prey. In addition, when the prey's growth rate is lower than the birth rate of the predator, global prey lattice formation is initiated by microlattices at the center of prey spirals. The predator lattice is later formed in the predator spirals. But both lattice formations proceed together as the prey growth rate increases.

DOI: 10.1103/PhysRevE.85.011915 PACS number(s): 87.18.−h, 87.10.−e, 87.23.−n

I. INTRODUCTION

The relationship between predator and prey populations is the most essential factor contributing to ecosystem conservation. As a result, predator-prey population dynamics has been extensively investigated since the study by Lotka and Vortella [1]. Since their pioneering work, many improved models have been proposed. One of them, by Rosenzweig and MacArthur (RM) [2], is adopted in this paper. Predator-prey systems have played an important role not only in ecology, but also in the study of general pattern formation. The most well-known case may be the discovery of chaos in population dynamics by May [3]. However, these works did not incorporate the spatial migration of predator and prey. On the other hand, Turing has pointed out the importance of diffusion in spatial pattern formation [4]. His activator-inhibitor scheme was later generalized mathematically as the reaction-diffusion theory by Meinhardt *et al.* [5] and successfully applied to various systems [6]. In the case of the predator-prey system, the migration of predator and prey appears mathematically as a form of diffusion. Thus, the spatial pattern formation of the predator-prey systems has been extensively investigated by using the reaction-diffusion scheme. Nonetheless, the role of diffusion in the predator-prey systems has not been clarified sufficiently well due to the high mathematical complexity of the scheme. Turing's idea is that stable spatial patterns can be produced when the diffusion of the inhibitor is larger than that of the activator. In the predator-prey systems, prey and predator should correspond to activator and inhibitor, respectively, based on their nature. However, to the author's knowledge, there have been no reports of a stable Turing pattern in realistic predator-prey systems, including the RM model [7–9]. Hassel *et al.* [10] reported on the stable Turing pattern in ecology only for the host-parasitoid system. Their work was based on the cellular automation model, which is an individual-based model (IBM) [11], not a reaction-diffusion model. To investigate this problem, we have recently proposed a stochastic model for the predator-prey system [12]. We have introduced the concept of stochastic diffusion into the IBM and succeeded in the reproduction of every pattern, including chaotic ones. However, the reproduction of Turing patterns was not successful. Thus, it is necessary to clarify the conditions necessary for the reproduction of the stable Turing pattern in a more systematic manner. In this paper, we adopt the realistic model by Rosenzweig and MacArthur, and subsequently search for the general conditions to reproduce the stable Turing pattern in a systematic manner. As a result of this procedure, we identified the specific domain for the stable lattice formation.

II. PHASE DIAGRAM OF PREDATOR-PREY SYSTEMS

To study the Turing pattern in predator-prey systems, we adopted the well-known model of Rosenzweig and MacArthur:

$$\begin{aligned} \frac{du}{dt} &= au\left(1-\frac{u}{k}\right)-\frac{buv}{c+u} \equiv f(u,v), \\ \frac{dv}{dt} &= \frac{muv}{c+u}-nv \equiv g(u,v), \end{aligned} \tag{1}$$

where u and v represent the population densities of prey and predator, a and k represent the growth rate and carrying capacity of the prey population, and b, c, m, and n represent the maximum uptake rate, half-saturation prey density, birth rate, and death rate of the predator, respectively. Since individual parameters have their distinct meanings, we can find the biological origin of various patterns.

To simplify our investigation, we defined the following variables: $u = kU$, $v = acV/b$, $k/c = \beta$, $\alpha = a/m$, $\gamma = n/m$, and $mt = T$. We could then reduce the number of parameters from six to three and derive the following equation:

$$\begin{aligned} \frac{dU}{dT} &= \alpha U\left[(1-U)-\frac{V}{1+\beta U}\right] \equiv F(U,V), \\ \frac{dV}{dT} &= V\left(\frac{\beta U}{1+\beta U}-\gamma\right) \equiv G(U,V). \end{aligned} \tag{2}$$

From a stability analysis of the above equation (see the Appendix for details), it was found that we could divide the γ-β space into the following three domains [as shown in Fig. 1(a)]: domain I where $0 < \beta \leqslant \beta_0(\gamma)$, domain II where $\beta_0(\gamma) < \beta \leqslant \beta_1(\gamma)$, and domain III where $\beta_1(\gamma) < \beta$, with $\beta_0(\gamma) = \gamma/(1-\gamma)$ and $\beta_1(\gamma) = (1+\gamma)/(1-\gamma)$. A later analysis showed that in the presence of animal migrations,

*nagano@sk.ritsumei.ac.jp

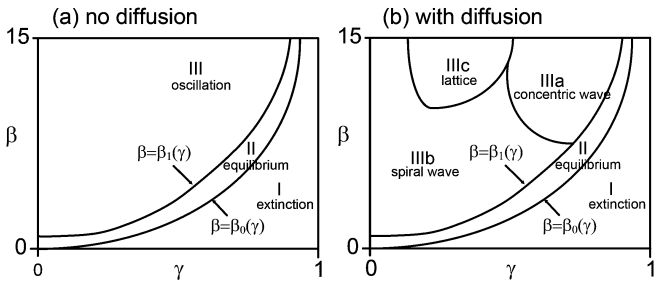

FIG. 1. Schematic phase diagram of pattern formation in the γ-β space. (a) No diffusion. In domain I, the predator population becomes extinct. In domain II, both predator and prey populations remain stable. In domain III, both predator and prey populations show stable oscillatory motion with some time lag between each other. (b) With diffusion. Domain III in (a) is divided into three subdomains. In domain IIIa, concentric waves of predator and prey appear in turn. In domain IIIb, both predator and prey populations show spiral patterns. In domain IIIc, stable predator and prey lattices are formed.

domain III is further divided into three subdomains, namely, IIIa, IIIb, and IIIc, as shown in Fig. 1(b).

First of all, adopting Eq. (2), we show the predator and prey populations as a function of time in Fig. 2. In domain I, the predator population becomes extinct; in domain II, both predator and prey populations remain stable; and in domain III, both predator and prey populations show stable oscillatory motion with some time lag between each other.

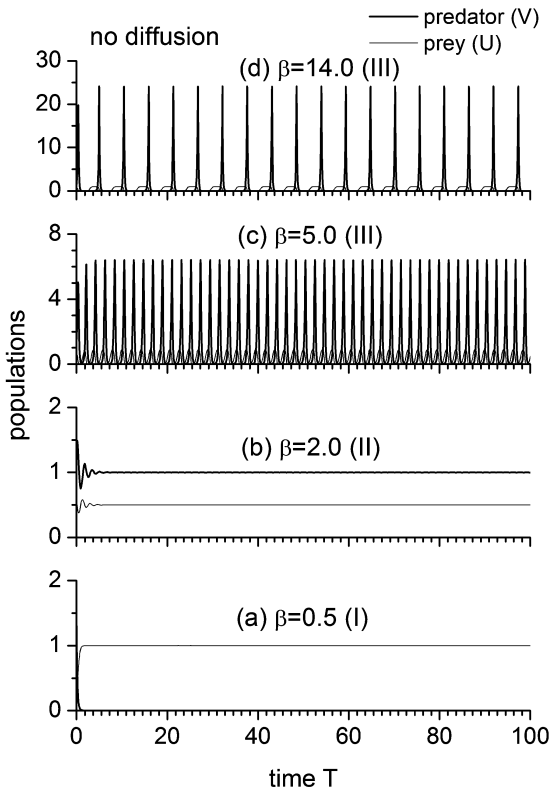

FIG. 2. Development of predator and prey populations over time without diffusion when $\alpha = 0.3$ and $\gamma = 0.5$, where $\beta = 0.5$ in domain I, $\beta = 2.0$ in domain II, and $\beta = 5.0$ and 14.0 in domain III.

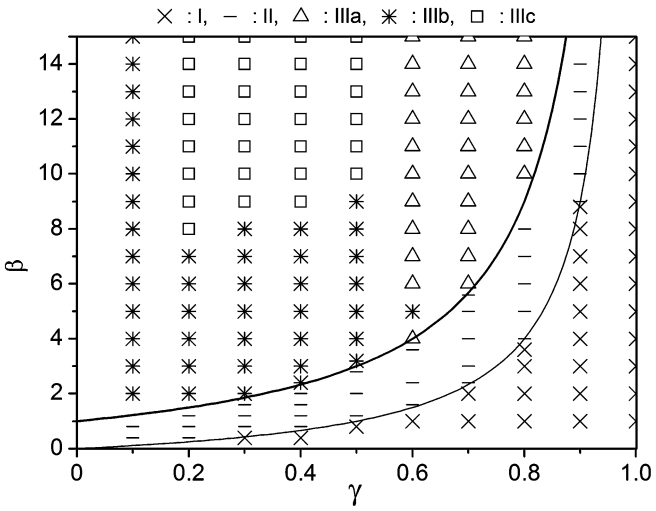

FIG. 3. Phase diagram for $\alpha = 0.3$, and $D_U \equiv D = 0.01$ and $D_V = 1$ in the γ-β space. When diffusion is introduced, domain III is further divided into three subdomains, namely, IIIa, IIIb, and IIIc. Periodic concentric waves and spiral waves appear in domains IIIa and IIIb, respectively, and stable lattice structures are formed in domain IIIc.

To investigate the role of diffusion in detail, we adopted the following equations:

$$\begin{aligned} \frac{dU}{dT} &= F(U,V) + D_U \nabla^2 U, \\ \frac{dV}{dT} &= G(U,V) + D_V \nabla^2 V, \end{aligned} \tag{3}$$

where $\nabla^2 = \partial^2/\partial x^2 + \partial^2/\partial y^2$, and D_U, D_V are diffusion coefficients of the prey and the predator, respectively. The effect of migration of the predator and prey was taken into account as a form of diffusion. We then studied the effect of diffusion by reducing the value of $D_U \equiv D$ from 1, with $D_V = 1$. We adopted this procedure only to maintain sufficient numerical accuracy throughout our study. Our extensive quantitative analysis showed that patterns in domains I and II were surprisingly unchanged, even after the introduction of diffusion terms. However, domain III could be further divided into three subdomains, i.e., IIIa, IIIb, and IIIc, as shown in Fig. 3, where we adopted $D = 0.01$ and $\alpha = 0.3$. With a decrease in γ, different patterns appeared one after another in domain III. Namely, the periodic concentric waves appeared in domain IIIa, and spiral waves or stable lattice patterns appeared in domains IIIb and IIIc, respectively. The patterns in domain IIIc were obviously those predicted by Turing. The border of domain IIIc expanded in the direction of smaller β values, with further decreases in the D value.

In Fig. 4, we show the corresponding average predator and prey population densities $\overline{V}$ and $\overline{U}$ as a function of time T when $D = 0.01$ and $\alpha = 0.3$.

Figure 5 shows the time development of the two-dimensional distribution of population densities of the corresponding cases in Fig. 4.

In Fig. 6, we show the time development of the average population densities in domain IIIa. For comparison, we also

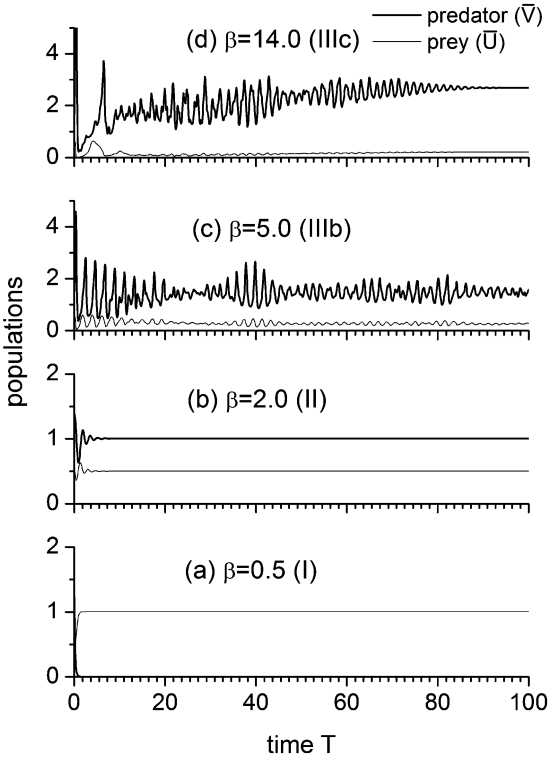

FIG. 4. Predator and prey population densities $\overline{V}$ and $\overline{U}$ as a function of time T in the four domains, where $D = 0.01, \alpha = 0.3, \gamma = 0.5$, and $\beta = 0.5$, 2.0, 5.0, and 14.0 in the domains I, II, IIIb, and IIIc, respectively.

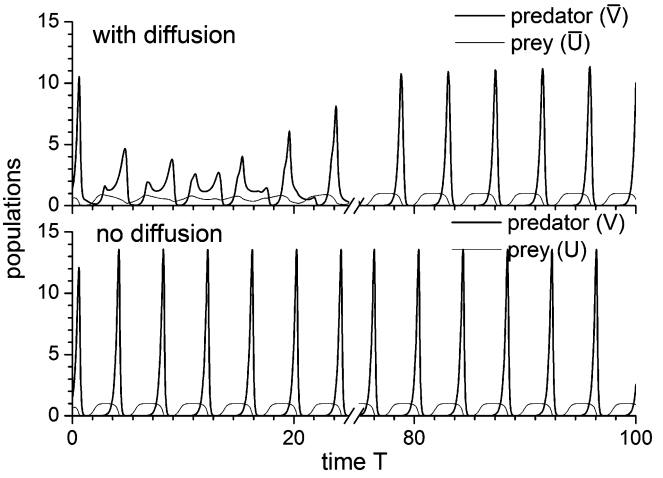

FIG. 6. Predator and prey population densities $\overline{V}$ and $\overline{U}$ as a function of time T in domain IIIa, where $D = 0.01, \alpha = 0.3, \beta = 14$, and $\gamma = 0.7$. For comparison, we show V and U for the corresponding case without diffusion. Both patterns are similar except for the oscillation period.

show the corresponding case without diffusion. Surprisingly, the two cases look similar.

We also show the spatial patterns in domain IIIa in Fig. 7. In domain IIIa, concentric waves of the predator and prey populations are produced in turn and oscillation centers are fixed.

We found that the microlattice structure in the centers of prey spirals, as indicated by the white arrow in Fig. 8, initiates global lattice formation when $\alpha = 0.3$. However, prey and

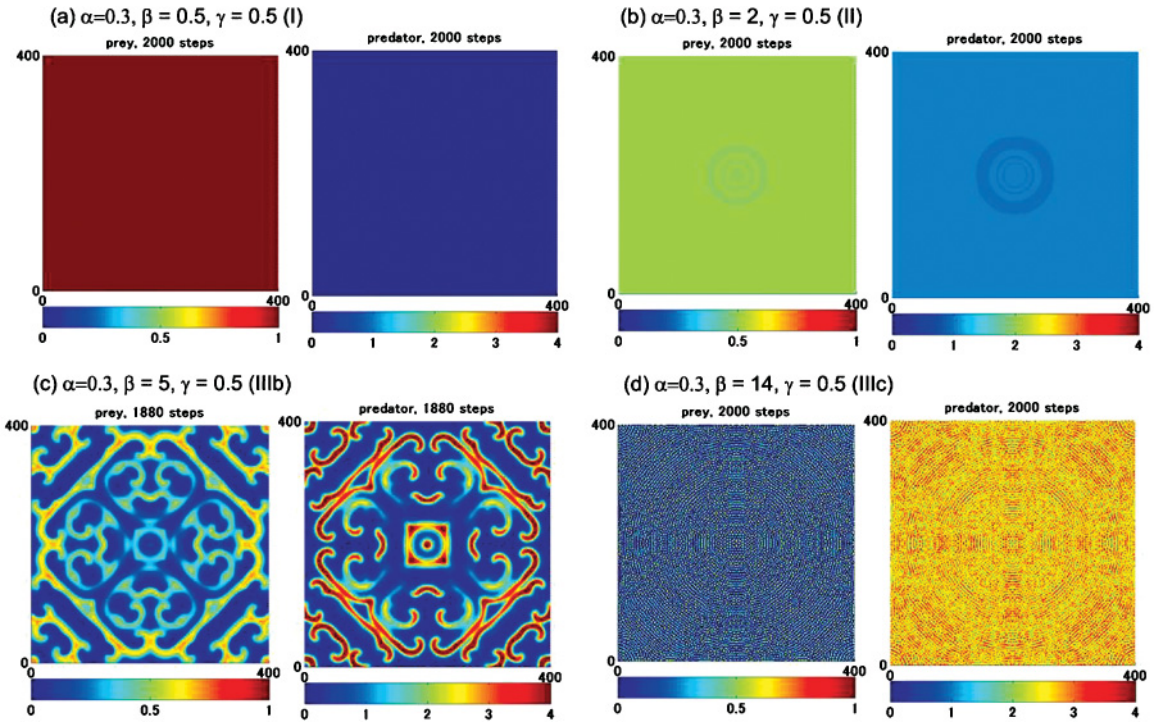

FIG. 5. (Color online) Predator and prey patterns in the four domains, i.e., I, II, IIIb, and IIIc. Here subtle patterns in domain II are dependent on the initial conditions. But the lattice structure in domain IIIc does not depend on the initial distribution. The time step for this simulation study is 0.05.

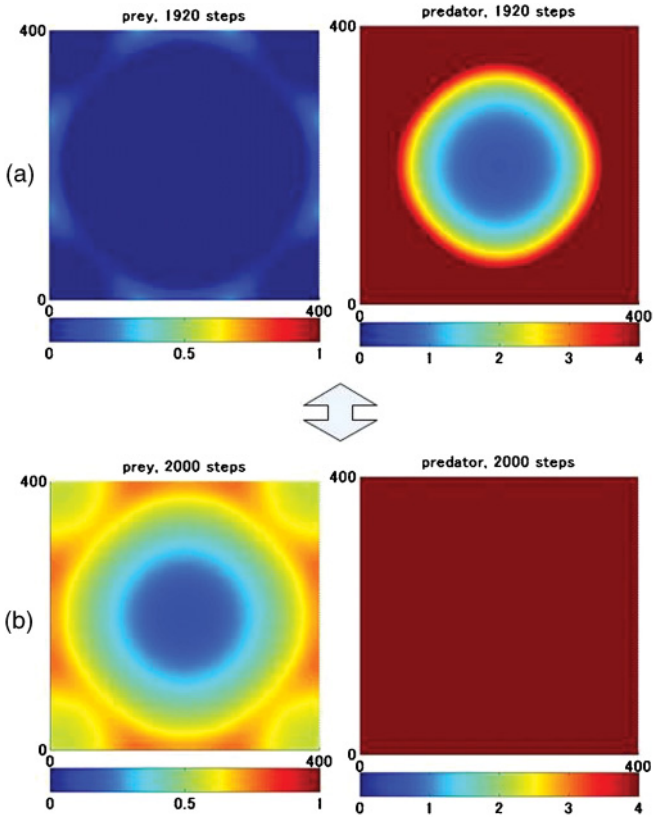

FIG. 7. (Color online) Concentric waves of predator and prey appear in turn in domain IIIa, where $\alpha = 0.3, \beta = 14$, and $\gamma = 0.7$. The time step is 0.05.

predator lattice formation proceeded together with an increase of α up to 1.0 in our study, as shown in Fig. 9.

When we started with uneven distributions of predator and prey, we always observed the above-mentioned pattern formation. However, only globally uniform oscillations appeared when the uniform, random, initial distributions of prey and predator were chosen. Figure 10 shows the average prey and predator oscillatory patterns of $\overline{V}$ and $\overline{U}$ in such a case.

Although there was no spatial variation of V and U, $\overline{V}$ and $\overline{U}$ in Fig. 10 are surprisingly similar to V and U in Fig. 2.

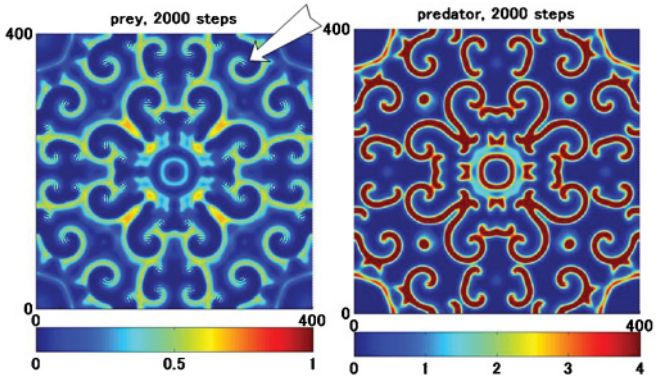

FIG. 8. (Color online) The prey microlattices in the centers of spirals are indicated by the white arrow; these initiate total crystallization when $\alpha = 0.3, \beta = 8$, and $\gamma = 0.5$. The time step is 0.05.

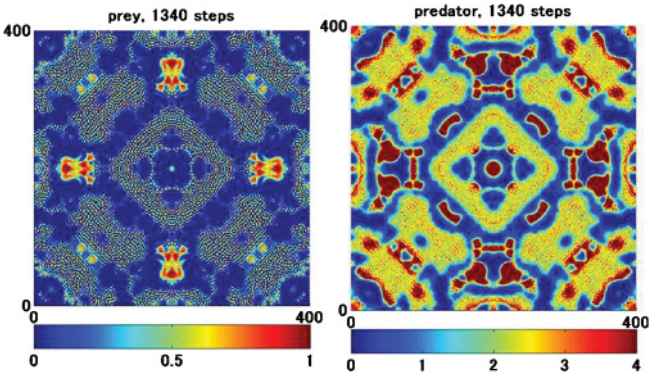

FIG. 9. (Color online) Lattice formation for prey and predator begins simultaneously when $\alpha = 0.5, \beta = 12$, and $\gamma = 0.5$. The time step is 0.05.

Specifically, it is hard to find the effect of diffusion. This is similar to what is observed with snowflake formation. It is known that a seed is necessary for snowflake formation, and the uneven predator and prey population seems to play the role of the seed in the current pattern formation.

III. ECOLOGICAL STABILITY

In this section, we apply our findings to the issue of ecological stability, which impacts a wide variety of phenomena, including, for example, locust outbreaks in Africa [13]. The

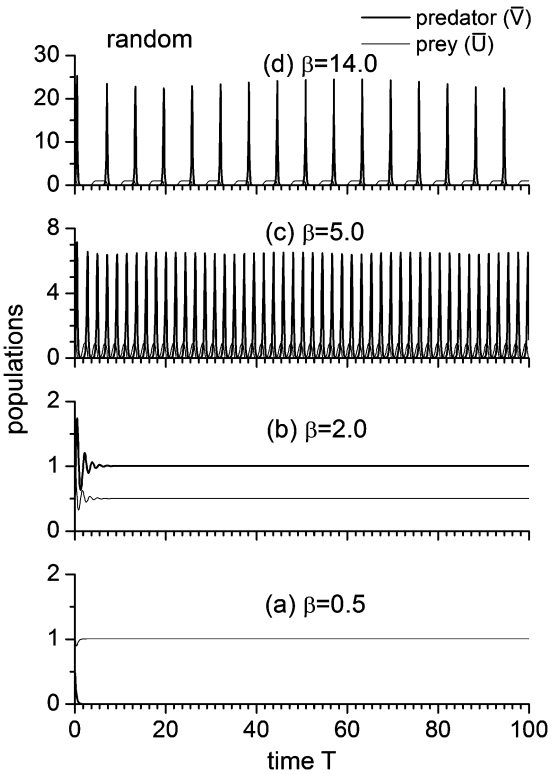

FIG. 10. With a uniform random distribution of the predator and prey populations, no specific pattern is formed, where $D = 0.01, \alpha = 0.3$, and $\gamma = 0.5$. Only spatially uniform patterns appear, and the development of the predator and prey populations over time is very similar to corresponding cases without diffusion.

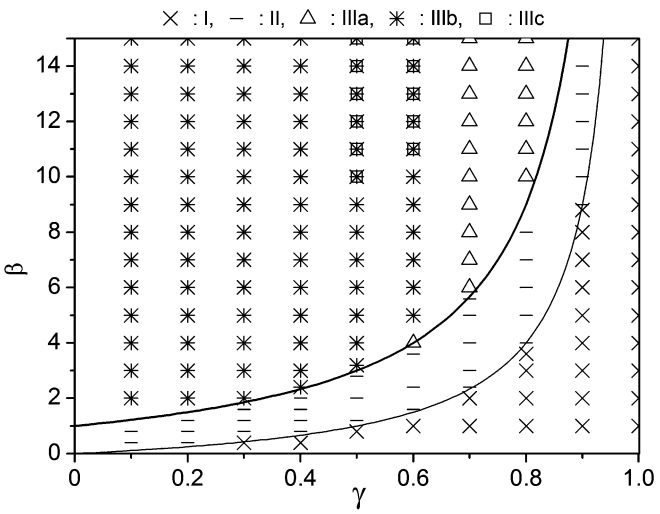

FIG. 11. Phase diagram for $\alpha = 0.1$ and $D = 0.01$. Spiral waves dominate domain III.

appearance of spiral patterns may not be favorable because the population dynamics demonstrate chaotic behavior, and the probability of predator extinction can increase as well. Thus, ecological stability can be expected in domains II, IIIa, and IIIc. To study this problem further, we investigated additional cases. Figure 11 shows the case where $\alpha = 0.1$, and Figs. 12 and 13 show the cases where $\alpha = 1.0$. In Figs. 12 and 13, $D = 0.01$ and $D = 0.03$, respectively. Domain IIIb, a chaotic area, expands its territory with an increase in α. On the other hand, domain IIIa, a concentric wave area, expands its border with a decrease in α. This means that larger values of $\alpha = a/m$ are favorable for ecological stability. Large α values mean that the growth rate of the prey, a, is larger than the birth rate of the predator, m. But in domain II, $\beta_0(\gamma) < \beta = k/c \leqslant \beta_1(\gamma)$, ecological stability does not depend on the α value at all. Here, $\beta \gg 1$, meaning that the carrying capacity of the prey population k is much larger than the half-saturation prey density c, and $\gamma \ll 1$ indicates that the birth rate of the predator m is much larger than the death rate of the predator n.

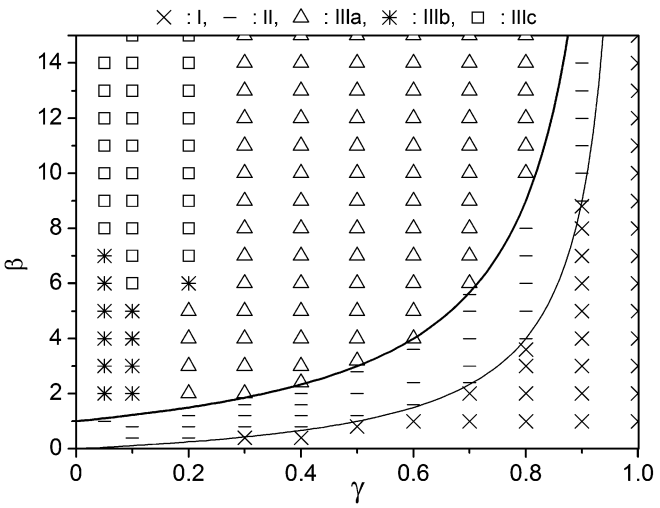

FIG. 12. Phase diagram for $\alpha = 1.0$ and $D = 0.01$. Concentric waves dominate domain III.

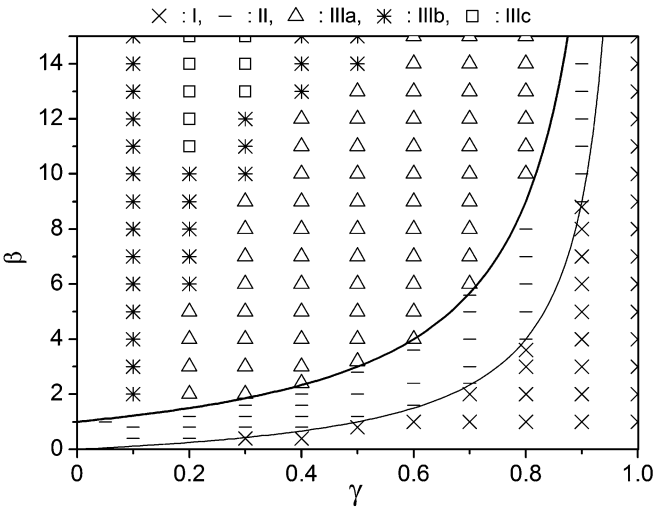

FIG. 13. Phase diagram for $\alpha = 1.0$ and $D = 0.03$. This figure is similar to Fig. 3. Compared to Fig. 3, however, concentric waves are more dominant than spiral waves in domain III.

IV. DISCUSSIONS

We found in our study that the γ-β space is appropriate for systematically classifying the pattern formation of the RM model as shown in Fig. 1. Figures 3, 11, 12, and 13, as well as other studies, show that the diffusion effect is suppressed when $\beta \leqslant \beta_1(\gamma)$, namely, in domains I and II. This is because $UV/(1+\beta U) \cong VU$, and $D\nabla^2 U$ becomes negligible compared to VU when $\beta U \gg 1$ and $V \gg 1$. However, domain III can be divided into three subdomains when the diffusion term is introduced. Lattice structures, namely, Turing patterns, are observed in domain IIIc, and spiral waves and periodic concentric waves are observed in domains IIIb and IIIa, respectively. According to our study, however, the simple activator-inhibitor scheme for the creation of stable patterns by Turing does not work here. Not only a small D value, but also a large carrying capacity for the prey k or small value of the half-saturation prey density c is needed for the production of the stable lattice structure. This is because the prey population decays according to $-\alpha UV/(1+\beta U)$, and thus the diffusion term $D\nabla^2 U$ can play a dominant role when the value of β $(=k/c)$ is sufficiently large.

Crystallization is initiated in the center of the prey spirals when the α value is small, as shown in Fig. 8. But with an increase in the α value, crystallization of the population

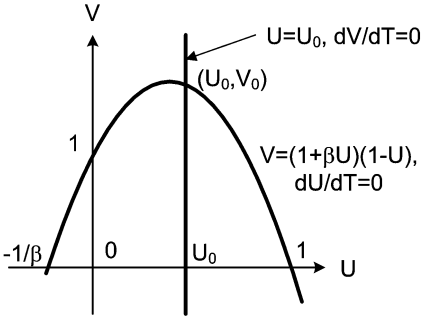

FIG. 14. Null lines $dU/dT = 0$ and $dV/dT = 0$. (U_0, V_0) is a stable point.

densities of the prey and predator proceeds together since the coupling between prey and predator becomes stronger, as shown in Fig. 9.

Similar patterns in the above phase diagrams can always be observed when uneven distribution of the predator and prey is chosen as their starting distributions. However, no matter how small a diffusion value D of the prey is chosen, only spatially uniform patterns appear when the initial distribution of the predator and prey is completely random. This is very similar to what is observed in snowflake formation. Namely, some seed is necessary for the initiation of the pattern formation. Furthermore, Fig. 10 shows that the oscillations of the average predator and prey population densities $\overline{V}$ and $\overline{U}$ as a function of time T are very similar to those of V and U without diffusion, despite the presence of diffusion.

Our study showed that ecological stability can be expected in domains II, IIIa, and IIIc. Although stable patterns can be expected in domains II and IIIa, ecological activity such as the births and deaths of animals continues as usual in these domains. Thus, life is not static in the static patterns.

APPENDIX: STABILITY ANALYSIS

Reaction null clines in the Rosenzweig and MacArthur model are $dU/dT = 0$ when $U = 0$, or $V = (1 + \beta U)(1 - U)$, and $dV/dT = 0$ when $U = U_0$, or $V = 0$. Furthermore $dU/dT = dV/dT = 0$ when $(U,V) = (U_0,V_0)$, or $(U,V) = (1,0)$, where $U_0 = \beta_0(\gamma)/\beta$, $V_0 = [1 - \beta_0(\gamma)/\beta]/(1 - \gamma)$, and $\beta_0 = \beta_0(\gamma) = \gamma/(1 - \gamma)$. We have $0 < \gamma < 1$ from $U_0 > 0$, and $\beta > \beta_0$ from $V_0 > 0$.

Expanding U,V at (U_0,V_0) as $U = U_0 + u, V = V_0 + v$, and keeping only linear terms of u,v, we obtain

$$\frac{d}{dT}\begin{pmatrix} u \\ v \end{pmatrix} = \begin{pmatrix} \alpha\gamma\,(\beta - \beta_1)/\beta & -\alpha\gamma/\beta \\ (1-\gamma)(\beta - \beta_0) & 0 \end{pmatrix}\begin{pmatrix} u \\ v \end{pmatrix} = A\begin{pmatrix} u \\ v \end{pmatrix}, \tag{A1}$$

where $\beta_0(\gamma) = 1/(1 - \gamma)$ and $\beta_1(\gamma) = (1 + \gamma)/(1 - \gamma)$. Eigenvalues of the matrix A are

$$\lambda_\pm = \frac{\tau \pm \sqrt{\tau^2 - 4\Delta}}{2}, \tag{A2}$$

where

$$\tau = \mathrm{tr}\,(A) = \frac{\alpha\gamma}{\beta}\,(\beta - \beta_1)\,,$$

$$\Delta = \det A = \frac{\alpha\gamma\,(1-\gamma)}{\beta}\,(\beta - \beta_0)\,.$$

Thus, (U_0,V_0) is a stable state when $\beta_0(\gamma) \leqslant \beta \leqslant \beta_1(\gamma)$ and $0 < \gamma < 1$. This is because $\tau \leqslant 0$ and $\Delta \geqslant 0$, and $\lambda_\pm$ becomes negative and both u and v vanish over time.

[1] J. D. Murray, *Mathematical Biology*, 3rd ed. (Springer-Verlag, Berlin-New York, 2001).

[2] M. L. Rosenzweig and R. H. MacArthur, Am. Nature **97**, 209 (1963).

[3] R. M. May, Nature (London) **261**, 459 (1976).

[4] A. M. Turing, Philos. Trans. R. Soc. London **327**, 37 (1952).

[5] A. J. Koch and H. Meinhardt, Rev. Mod. Phys. **66**, 1481 (1994).

[6] P. K. Maini, K. J. Painter, and H. N. P. Chau, J. Chem. Soc. Faraday Trans. **93**, 3601 (1997).

[7] W. S. C. Gurney, A. R. Veitch, I. Cruickshank, and G. McGeachin, Ecology **79**, 2516 (1998).

[8] M. V. Carneiro and I. C. Charret, Phys. Rev. E **76**, 0619021 (2007).

[9] M. R. Garvie and C. Trenchea, J. Biol. Dyn. **4**, 559 (2010).

[10] M. P. Hassell, H. N. Comins, and R. M. May, Nature (London) **353**, 255 (1991).

[11] D. L. DeAngelis and D. D. Mooij, Annu. Rev. Ecol. Evol. Syst. **36**, 147 (2005).

[12] A. Yokoyama, Y. Noguchi, and S. Nagano, J. Biol. Phys. **34**, 121 (2008).

[13] M. C. Todd, R. Washington, R. A. Cheke, and D. Kniveton, J. Appl. Ecol. **39**, 31 (2002).